

Diameter selective reaction processes of single-wall carbon nanotubesF. Simon, Á. Kukovecz,* C. Kramberger, R. Pfeiffer, F. Hasi, and H. Kuzmany
Institut für Materialphysik, Universität Wien, Strudlhofgasse 4, A-1090 Wien, Austria

H. Kataura

Department of Physics, Tokyo Metropolitan University, Tokyo, Japan

(Received 11 November 2004; published 29 April 2005)

A method is presented which allows the study of diameter selective reactions in single-wall carbon nanotubes with an unprecedented accuracy. It is based on the transformation of fullerene peapods into double-wall carbon nanotubes and the study of the resulting diameter distribution of the inner nanotubes with Raman spectroscopy. This yields a spectral resolution increase of about 40 for the modes of different tubes. The method is demonstrated for the diameter selective healing of nanotube defects and yield from C_{70} peapod samples. The growth of very small diameter inner tubes from C_{70} peapods is demonstrated, which challenges the models of inner nanotube formation. An anomalous absence of middiameter inner tubes is explained by the suppressed amount of C_{70} peapods in the transition region between standing and lying C_{70} configurations.

DOI: 10.1103/PhysRevB.71.165439

PACS number(s): 61.46.+w, 78.30.Na

I. INTRODUCTION

Nanostructures based on carbon nanotubes¹ have been in the forefront of nanomaterial research in the past decade. However, there still remains a number of open questions before one of the most promising candidates, namely single-wall carbon nanotubes (SWCNTs), will have wide-spread applications. The major obstacle is the large number of electronically different nanotubes produced with varying diameters and chiralities.² Directed growth or separation efforts are hindered by the lack of accurate chiral vector identification methods in bulk samples. In addition, little is known about chirality and diameter sensitive reactions. Band-gap fluorescence was successfully applied to assign chiral indices to semiconducting SWCNTs.³ Similarly, assignment of small diameter nanotubes to chiral vectors was performed in double-wall carbon nanotubes (DWCNTs) using Raman spectroscopy.^{4,5} DWCNTs are SWCNTs containing a coaxial, smaller diameter CNT. The material is produced from fullerenes encapsulated in SWCNT (peapods⁶) by a high-temperature treatment.⁷ The growth process in such systems is of fundamental interest, since it proceeds without catalytic particle support.

The growth process of DWCNTs from fullerene peapods is not yet understood. Computer simulations have suggested that C_{60} @SWCNT based DWCNTs are formed by Stone-Wales transformations from C_{60} dimer precursors at high temperature by cycloaddition.^{8,9} The free rotation of C_{60} molecules is a prerequisite for the dimer formation as it enables the molecules to have facing double bonds. The ellipsoidal shaped C_{70} were found to be present in both standing or lying configurations, i.e., with the longer C_{70} axis perpendicular or parallel to the tube axis.^{10,11}

At first glance, the above-mentioned assignment by Raman spectroscopy of the inner tubes in DWCNTs is not applicable to study properties of the outer tubes. However, we show in this paper that the assignment of chiralities to the inner tubes of DWCNTs is a new and so far unique tool for a diameter selective or even chirality selective analysis of the

outer tube reactions. This possibility originates from the correlation between inner and outer tube abundances and from the robustness of this correlation against the different types of SWCNTs used for the inner tube growth. Due to the larger spectral splitting and narrower linewidths of the inner tube radial breathing modes,⁴ the inner tube diameter distribution can be characterized with a spectral resolution that is about 40 times larger as compared to the analysis of the outer tubes. Thus, the analysis of the inner tubes allows the characterization of diameter selective reactions in the starting material with an unprecedented accuracy. The method is demonstrated on the diameter selective healing of the SWCNT openings. A dramatic exception in the equivalency of the C_{60} and C_{70} grown tubes is also presented for the $d \approx 0.67$ nm inner nanotubes for which the corresponding outer tubes are on the border between lying and standing C_{70} configurations.

II. EXPERIMENTAL DETAILS

C_{60} and C_{70} based DWCNTs (60-DWCNT and 70-DWCNT, respectively) were prepared from two arc-discharge grown commercial SWCNTs (SWCNT-N1 and N2 from Nanocarlab, Russia) and two laser ablation grown tubes. From the latter, one was commercial (SWCNT-R from Tubes@Rice, Houston, TX) and the other was laboratory-prepared (SWCNT-L). The SWCNT-N1,N2 materials were purified to 50% by the manufacturer. SWCNT-R and SWCNT-L materials were purified following Ref. 12. Peapod samples were prepared by annealing SWCNT with C_{60} in a quartz tube following Ref. 12 and were transformed to DWCNT at high temperature following Ref. 7. The diameter distributions of the SWCNT materials were determined from Raman spectroscopy¹³ giving $d_{N1}=1.50$ nm, $\sigma_{N1}=0.10$ nm, $d_{N2}=1.45$ nm, $\sigma_{N2}=0.10$ nm, $d_R=1.35$ nm, $\sigma_R=0.09$ nm, and $d_L=1.39$ nm, $\sigma_L=0.09$ nm for the mean diameters and the variances of the distributions, respectively. The results described here were observed for all samples. Multifre-

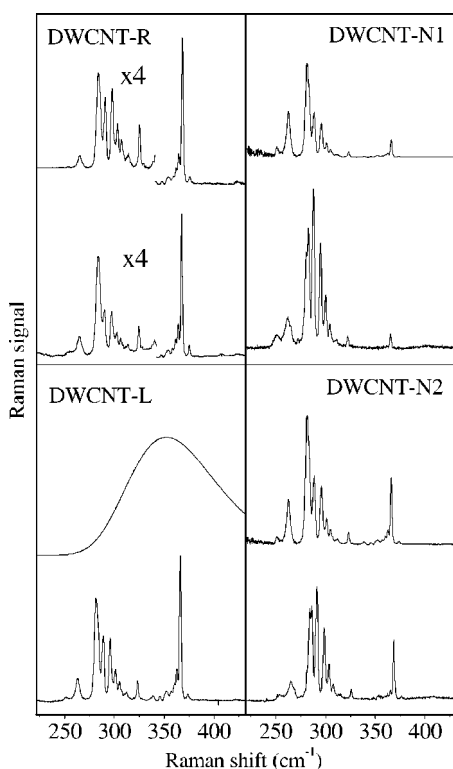


FIG. 1. As measured Raman spectra of the inner nanotube RBMs for four 60-DWCNT samples (lower curves in each quarter) at $\lambda=647$ nm laser excitation. The upper spectra are smart scaled from the lower left spectrum. The Gaussian diameter distribution is shown for the DWCNT-L sample.

quency Raman spectroscopy was performed on a Dilor xy triple axis spectrometer in the 1.64–2.54 eV (755–488 nm) energy range and in a Bruker FT-Raman spectrometer for the 1.16 eV (1064 nm) excitation at 90 K. The spectral resolution was 1–2 cm^{-1} depending on the laser wavelength. Raman shifts were calibrated against a series of spectral calibration lamps.

III. EXPERIMENTAL RESULTS AND DISCUSSION

In Fig. 1, we compare Raman spectra of the different 60-DWCNT materials for the 647 nm excitation. The spectra are representative for excitations with other laser energies and represent the response from the radial breathing mode (RBM) of inner tubes. The RBMs of all the observable inner tubes, including the split components,⁴ can be found at the same position in all DWCNT samples within the ± 0.5 cm^{-1} experimental precision of our measurement for the whole laser energy range studied here. This proves that vibrational modes of DWCNT samples are robust against the starting material.

As the four samples have different diameter distributions, the overall Raman patterns look different. However, scaling the patterns with the ratio of the distribution functions (smart scaling) allows us to generate the overall pattern for all systems, starting from, e.g., DWCNT-L in the bottom-left corner of Fig. 1. It was assumed that the inner tube diameter distri-

butions follow a Gaussian function with a mean diameter 0.72 nm smaller than those of the outer tubes¹⁴ and with the same variance as the outer tubes. We used the empirical constants from Ref. 5 for the RBM mode Raman shift versus inner tube diameter expression. The corresponding Gaussian diameter distribution of inner tubes is shown for the DWCNT-L sample in Fig. 1. We observe a good agreement between the experimental and simulated patterns for the DWCNT-R sample. A somewhat less accurate agreement is observed for the DWCNT-N1,N2 samples, which may be related to the different growth method: arc discharge for the latter, as compared to laser ablation for the R and L samples. The observed agreement has important consequences for the understanding of the inner tube properties. As a result of the photoselectivity of the Raman experiment, it proves that the electronic structure of the inner tubes is identical in the different starting SWCNT materials.

The RBM frequencies of neighboring inner tubes are on the average four times more separated from each other than those of the outer ones.⁵ In addition, the outer tube RBMs have a typical full width at half maximum (FWHM) of 5–10 cm^{-1} (Ref. 15) as compared to the FWHM of the inner tube RBMs of 0.5 cm^{-1} (Ref. 4). As a result, the available spectral resolution is at least 40 times larger when the RBMs of the inner tubes are investigated. This allows us to study chirality or at least diameter selective reactions of the outer tubes by analyzing the inner tube response.

In Fig. 2, we show the Raman spectra of the 60-DWCNT-N2 heat-treated at 800 °C in dynamic vacuum for 40 min prior to the C_{60} encapsulation and DWCNT transformation as compared to an untreated sample. The spectra are normalized by the amplitude of the corresponding outer tubes. The weaker response at higher Raman shifted lines, i.e., inner tubes with smaller diameters, is apparent in Fig. 2(b) and is shown quantitatively in Fig. 2(c). The result is evidence for an annealing induced closing of the outer tubes with small diameters, which prevents the C_{60} encapsulation. It relates to the higher reactivity for healing of openings in small diameter SWCNTs, which provide the host for the narrower inner tubes. To exclude other effects, such as coalescence observed at similar temperatures under intensive electron radiation,¹⁶ we checked that the full inner tube signal can be obtained for samples subject to a 30-min-long 500 °C oxidation treatment in air (reopening) after the vacuum annealing. Although the overall healing effect and the more rapid closing of smaller nanotubes has been long anticipated, to our knowledge this is the first example when it is observed with an individual tube sensitivity. The technique allows a quantitative determination of the healing speed of the different SWCNTs.

Figure 3 compares the Raman spectra of 60- and 70-DWCNT-R for some representative laser energies. The RBMs of all the observable inner tubes, including the split components, can be found at the same position for all the 60-DWCNT and 70-DWCNT samples within our experimental precision. This reinforces the previous finding that the inner tube formation is robust against the starting SWCNT material or fullerene. The spectra shown in Fig. 3 are pairwise normalized by the intensity of a selected inner tube from the 300–340 cm^{-1} spectral range.

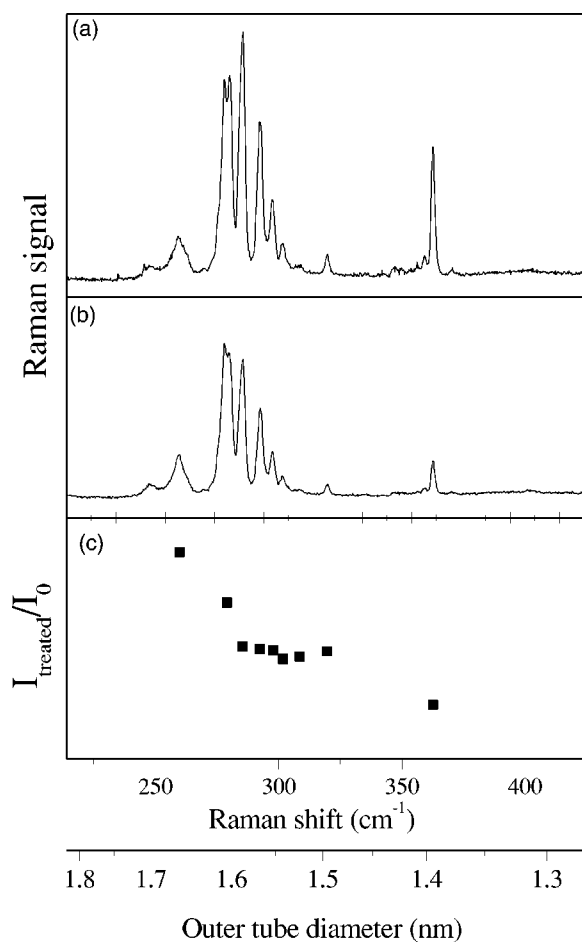


FIG. 2. Raman spectra of untreated tubes (a), tubes heated at 800 °C prior to filling (b), and ratio of the inner tube signal intensity for the heat treated (I_{treated}) and the untreated material (I_0) (c). The lowest scale shows the diameters of the corresponding outer tubes.

The observation of the very small inner tubes, with Raman shifts ranging up to 450 cm⁻¹ for 70-DWCNTs, is important. The smallest observable inner tubes for 60-SWCNT were found to be⁴ the (7,0), (5,3), (4,4), and (6,1) with diameters of 0.553, 0.553, 0.547, and 0.519 nm, respectively.⁵ As indicated by solid arrows in Fig. 3, we clearly observe the (7,0), (5,3), and (4,4) for the 70-DWCNT-R sample with intensities similar to those in 60-DWCNT. The identification of the (6,1) tube is less certain as it appears with very small intensity already for the 60-DWCNT sample in a previous report.⁴ Using the experimentally determined 0.72 nm inner and outer tube diameter difference,¹⁴ the cutoff of the inner tube distribution at the (6,1) tube for 60-DWCNT can be related to the smallest outer tube with $d_{\text{cutoff},C_{60}} \approx 1.239$ nm where C_{60} can enter. This value is in reasonable agreement with theoretical estimates where $d_{\text{cutoff},C_{60}} \approx 1.2$ nm was found for the smallest tube diameter where C_{60} peapod formation is energetically favored.¹⁷⁻¹⁹ Similarly, the energetics of the C_{70} encapsulation was calculated and $d_{\text{critical}} \approx 1.35$ nm was found for the SWCNT diameter, which separates the standing and lying configurations.²⁰ Based on this value, inner tubes with $d \leq 0.63$ nm can only be formed from

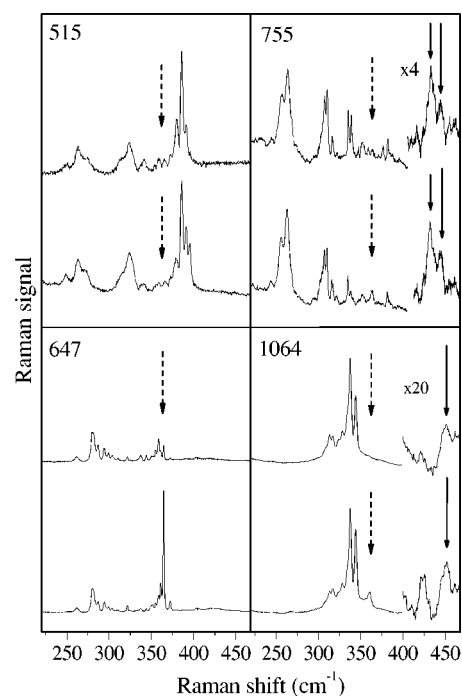


FIG. 3. Comparison of the Raman spectra of 60-DWCNT-R (lower spectra) and 70-DWCNT-R (upper spectra) for $\lambda = 515, 647, 755,$ and 1064 nm, respectively. Solid arrows indicate the (7,5) and (5,3) nanotubes in the 755 nm spectra and the (4,4) nanotube on the 1064 spectra. Dashed arrows mark the vicinity of the 362 ± 3 cm⁻¹ spectral range.

C_{70} peapods in the lying configuration. The diameters of the above-mentioned and arrow-indicated tubes in Fig. 3 are all well below this value. Thus, the smallest observed inner tubes for the 70-DWCNT are made nominally from lying C_{70} peapod molecules.

The above result has important implications on the theoretical models of the inner tube formation. It has been suggested that the route to inner tube growth is the formation of cycloadditionally bonded precursor C_{60} dimers.^{8,9} Once the dimers are formed, Stone-Wales transformations proceed until the completely formed inner tubes are developed. As cycloaddition needs facing parallel double bonds, the lying C_{70} molecules are geometrically hindered to establish this reaction due to the facing pentagons.² Therefore, a different process must be anticipated for the formation of very small diameter inner tubes. This means the theory of inner tube formation requires revision. As an alternative possibility for the formation of inner tubes, a complete decay of the fullerenes into, e.g., C_2 units may take place. In this case, the particular geometry of the given fullerene does not play a role.

In what follows, an anomalous behavior observed for 70-DWCNTs with $d_{\text{outer}} \approx d_{\text{critical}}$ is discussed. The dashed arrows in Fig. 3 mark the vicinity of the 363 ± 3 cm⁻¹ Raman shifted RBMs which were previously identified to originate from the (5,5) metallic ($d = 0.68$ nm) and the (8,1) semiconducting ($d = 0.671$ nm) inner tubes along with their split components.^{4,5} For the 647 nm excitation, an unusual and unexpected behavior is observed. Within the Raman shift

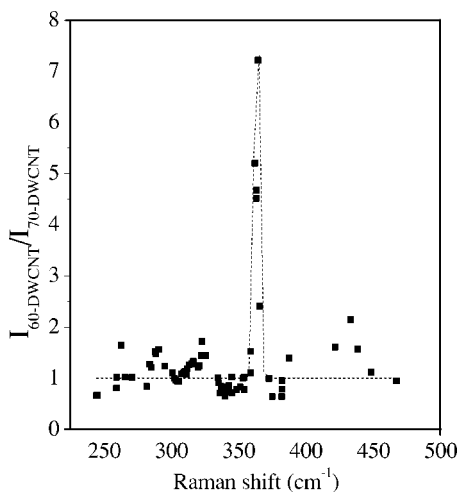


FIG. 4. Normalized intensity ratios of the Raman RBM modes of inner tubes in 60-, and 70-DWCNT-R materials at all laser lines studied. The data are sliding averaged as explained in the text. The dashed curve is a guide to the eye.

range indicated by the dashed arrows, some inner tube RBM components are significantly weaker for the 70-DWCNT samples as compared to the 60-DWCNT samples. This is consistent with the results of the 755 and 1064 nm excitations where weaker RBM modes are observed for the 70-DWCNT-R sample. The spectra recorded for 515 nm excitation did not exhibit a relevant signal in the Raman shift region under discussion.⁴ The same anomalous behavior was observed for 70-DWCNT samples prepared from other SWCNT materials.

To quantify this effect, we compared the intensity ratio of the inner tube RBMs in 60- and 70-DWCNTs for all measured laser lines and for all observed tubes. Voigtian lines were fitted to the observed spectra with a Gaussian width determined by the spectrometer response to the elastically scattered light and with a Lorentzian linewidth of the corresponding RBM mode. As discussed above, we chose a particular tube in the $300\text{--}340\text{ cm}^{-1}$ spectral range to normalize the observed inner tube RBM intensities before dividing the so-obtained values for the 60- and 70-DWCNTs by each other. Data points were collected for the RBM from each tube for excitations with eight different lasers and smoothed with three-point sliding averaging. This procedure reduces the noise of the intensity ratio and makes a data point more reliable when the same tube is observed at different laser energies. The result is summarized in Fig. 4. The anomaly of the intensity ratio is clearly observed in the $363\pm 3\text{ cm}^{-1}$ spectral range. This spectral range corresponds to inner tubes with $d_{\text{inner}}\approx 0.67\text{ nm}$ and $d_{\text{outer}}\approx 1.39\text{ nm}$. As the latter value is close to the critical diameter, it is tempting to associate the anomaly with the competition between the two configurations. In this case, the critical diameter to allow for standing C_{70} encapsulates is refined by the experiment to 1.39 nm. We

discuss two possible origins of the missing inner tubes: (i) inability to form inner tubes from peapods filled with mixed lying and standing C_{70} configurations, (ii) inability of C_{70} to enter into SWCNTs with $d_{\text{outer}}\approx d_{\text{critical}}$. Concerning the first case, SWCNTs with $d_{\text{outer}}\approx d_{\text{critical}}$ can be filled with mixed lying and standing C_{70} molecules, which makes a cycloaddition reaction difficult. However, we have shown that inner tubes are also formed from lying C_{70} molecules alone, which disfavors the idea that the precursor dimer is indeed necessary for the inner tube formation. Thus, it is argued that the absence of inner tubes when $d_{\text{outer}}\approx d_{\text{critical}}$ is rather caused by the absence of C_{70} molecules for peapods with this diameter.

A mechanism involving impurities or side-wall defects can explain the following observation: for the critical outer tube diameter, one can expect that for a perfect tube the lying configuration is preferred. However, when side-wall defects or impurities are present, a C_{70} may change its configuration to a standing geometry that would immobilize it, thus preventing other C_{70} from entering the tube. Alternatively, a C_{70} molecule entering at the critical diameter may get trapped at a tube defect as, e.g., a bend or kink and thus prevents further filling. The diameter selective filling may provide a way to mass-separate the unfilled and filled C_{70} peapod tubes. Interestingly, the outer tubes which remain unfilled are close to the well studied (10,10) tube.

IV. CONCLUSIONS

In conclusion, DWCNT formation from peapods enables the study of diameter selective phenomena in SWCNT materials. The method provides a new and accurate tool for the characterization of controlled nanotube growth and the effects of subsequent treatments or diameter selective separation. The diameter selective closing of tube openings was observed for the first time. Comparison of C_{60} , C_{70} peapod based DWCNTs proves that the inner tube formation is a conservative process against the starting SWCNT or fullerene material. The presence of very small inner nanotubes in 70-DWCNT presents a challenge to the current theoretical models. The absence of middiameter inner tubes in 70-DWCNT is explained by the absence of C_{70} peapods for the corresponding nanotube diameter due to the borderline between the lying and standing C_{70} configurations.

ACKNOWLEDGMENTS

Support from the FWF No. 14893, the EU NANOTEMP BIN2-2001-00580 and PATONN MEIF-CT-2003-501099 grants, the Hungarian State Grant No. OTKA F46361, and from the Industrial Technology Research Grant Program in '03 from the NEDO of Japan is acknowledged. Á.K. acknowledges support from the AMFK Foundation in the framework of the Zoltán Magyar programme.

*Present address: Department of Applied & Environmental Chemistry, University of Szeged, Hungary.

- ¹S. Iijima, *Nature (London)* **354**, 56 (1991).
- ²M. S. Dresselhaus, G. Dresselhaus, and P. C. Ecklund: *Science of Fullerenes and Carbon Nanotubes* (Academic Press, San Diego, 1996).
- ³S. M. Bachilo, M. S. Strano, C. Kittrell, R. H. Hauge, R. E. Smalley, and R. B. Weisman, *Science* **298**, 2361 (2002).
- ⁴R. Pfeiffer, H. Kuzmany, C. Kramberger, C. Schaman, T. Pichler, H. Kataura, Y. Achiba, J. Kürti, and V. Zólyomi, *Phys. Rev. Lett.* **90**, 225501 (2003).
- ⁵Ch. Kramberger, R. Pfeiffer, H. Kuzmany, V. Zólyomi, and J. Kürti, *Phys. Rev. B* **68**, 235404 (2003).
- ⁶B. W. Smith, M. Monthieux, and D. E. Luzzi, *Nature (London)* **396**, 323 (1998).
- ⁷S. Bandow, M. Takizawa, K. Hirahara, M. Yudasaka, and S. Iijima, *Chem. Phys. Lett.* **337**, 48 (2001).
- ⁸S. Han, M. Yoon, S. Berber, N. Park, E. Osawa, J. Ihm, and D. Tománek, *Phys. Rev. B* **70**, 113402 (2004).
- ⁹Y. Zhao, B. I. Yakobson, and R. E. Smalley, *Phys. Rev. Lett.* **88**, 185501 (2002).
- ¹⁰K. Hirahara, S. Bandow, K. Suenaga, H. Kato, T. Okazaki, H. Shinohara, and S. Iijima, *Phys. Rev. B* **64**, 115420 (2001).
- ¹¹H. Kataura, Y. Maniwa, M. Abe, A. Fujiwara, T. Kodama, K. Kikuchi, H. Imahori, Y. Misaki, S. Suzuki, and Y. Achiba, *Appl. Phys. A: Mater. Sci. Process.* **74**, 349 (2002).
- ¹²H. Kataura, Y. Maniwa, T. Kodama, K. Kikuchi, K. Hirahara, K. Suenaga, S. Iijima, S. Suzuki, Y. Achiba, and W. Krätschmer, *Synth. Met.* **121**, 1195 (2001).
- ¹³H. Kuzmany, W. Plank, M. Hulman, C. Kramberger, A. Gruneis, T. Pichler, H. Peterlik, H. Kataura, and Y. Achiba, *Eur. Phys. J. B* **22**, 307 (2001).
- ¹⁴M. Abe, H. Kataura, H. Kira, T. Kodama, S. Suzuki, Y. Achiba, K. I. Kato, M. Takata, A. Fujiwara, K. Matsuda, and Y. Maniwa, *Phys. Rev. B* **68**, 041405(R) (2003).
- ¹⁵A. Jorio, R. Saito, J. H. Hafner, C. M. Lieber, M. Hunter, T. McClure, G. Dresselhaus, and M. S. Dresselhaus, *Phys. Rev. Lett.* **86**, 1118 (2001).
- ¹⁶M. Terrones, H. Terrones, F. Banhart, J. C. Charlier, and P. M. Ajayan, *Science* **288**, 1226 (2000).
- ¹⁷M. Melle-Franco, H. Kuzmany, and F. Zerbetto, *J. Phys. Chem. B* **109**, 6986 (2003).
- ¹⁸S. Berber, Y-K. Kwon, and D. Tománek, *Phys. Rev. Lett.* **88**, 185502 (2002).
- ¹⁹M. Otani, S. Okada, and A. Oshiyama, *Phys. Rev. B* **68**, 125424 (2003).
- ²⁰S. Okada, M. Otani, and A. Oshiyama, *New J. Phys.* **5**, 122 (2003).